Article
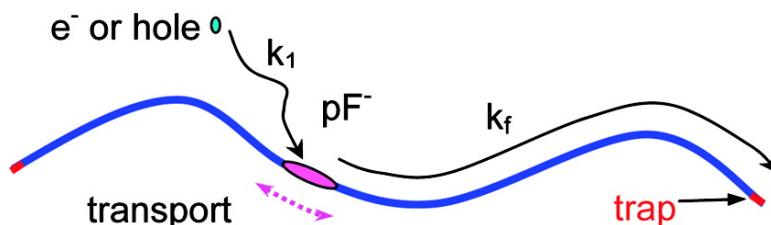
Electron and Hole Transport To Trap Groups at the Ends of Conjugated Polyfluorenes

Sadayuki Asaoka, Norihiko Takeda, Tomokazu Iyoda, Andrew R. Cook, and John R. Miller

More About This Article

Additional resources and features associated with this article are available within the HTML version:

- Supporting Information
- Access to high resolution figures
- Links to articles and content related to this article
- Copyright permission to reproduce figures and/or text from this article

View the Full Text HTML

Electron and Hole Transport To Trap Groups at the Ends of Conjugated Polyfluorenes

Sadayuki Asaoka, Norihiko Takeda, Tomokazu Iyoda, Andrew R. Cook, and
John R. Miller*

Chemistry Department, Brookhaven National Laboratory, Upton, New York 11973-5000

Received January 18, 2008; E-mail: jrmiller@bnl.gov

Abstract: Polyfluorenes (pF) were synthesized having anthraquinone (AQ) or naphtylimide (NI) end caps that trap electrons or di-p-tolylaminophenyl (APT$_2$) caps that trap holes. The average lengths of the pF chains in these molecules varied from 7 to 30 nm. End capping was found not to be complete in these molecules so that some were without caps. Electrons or holes were injected into these polymers in solution by pulse radiolysis. Following attachment, the charges migrated to the end cap traps in times near 2 ns in pF$_{12}$AQ or 5 ns in pF$_{35}$NI. From these observations, electron mobilities for transport along single chains to the end caps in THF solution were determined to be smaller by a factor of 100 than those observed by microwave conductivity. Despite this, the mobilities were sufficiently large to provide encouragement to the use of such single chains in solar photovoltaics. Most charges were observed to transport over substantial distances in these polymers, but 23, 18, and 37% of the charges attached to pFNI, pFAQ, and pFAPT$_2$, respectively, were trapped in the pF chains and decayed by slower bimolecular reactions. For pFAQ and pFAPT$_2$, all of the trapped charges were accounted for by estimates of the fraction of molecules having no end cap traps. For pF$_{35}$NI, 23% of the attached electrons were found to be trapped in the chains, but only 4% of chains were expected to have no end caps. This could indicate some trapping by kinks or other defects but may just reflect uncertainties in the capping of this long polymer. When the charges reach the trap groups, their spectra have no features of pF$^{\bullet-}$ or pF$^{\bullet+}$, nor do the principal bands of the trapped ions resemble spectra of the radical ions of isolated trap molecules. The optical absorption spectra are rather dominated by new bands identified as charge-transfer transitions, which probably reinject electrons or holes into the pF chains. The energies of those bands correlate well with measured redox potentials.

Introduction

Knowledge of transport in conjugated polymers could aid design of new low-cost nanostructured photovoltaics with structural control over length scales and molecular control of the direction of charge flow. Successful "plastic solar" cells with power conversion efficiencies approaching 5%[1–3] have been based on "bulk heterojunctions". Typical cells consist of ~50−50 mixtures of electron donors and acceptors in films that are usually random and unstructured. The close contact of acceptors with donors, usually conjugated polymers, eliminates the need for exciton transport over substantial distances, but low mobility of the separated charges is a barrier to high efficiency[3–6] and limits freedom to alter the energetics of the acceptor. High charge mobilites could break barriers to high efficiencies, and therefore approaches to improved mobilities have been explored.[7–11] Especially important and intriguing

have been the findings of Warman and co-workers at Delft. They measured charge motion within single polymer chains in solution by microwave conductivity;[12–16] they found mobilities much higher than those typical in films[4,17–19] and noted that interchain

(1) Reyes-Reyes, M.; Kim, K.; Carroll, D. L. *Appl. Phys. Lett.* **2005**, *87*, 083506.
(2) Kim, J. Y.; Kim, S. H.; Lee, H.-H.; Lee, K.; Ma, W. L.; Gong, X.; Heeger, A. J. *Adv. Mater.* **2006**, *18*, 572–576.
(3) Gunes, S.; Neugebauer, H.; Sariciftci, N. S. *Chem. Rev.* **2007**, *107*, 1324–1338.
(4) Huynh, W. U.; Dittmer, J. J.; Alivisatos, A. P. *Science* **2002**, *295*, 2425–2427.
(5) Nunzi, J. M. *C. R. Phys.* **2002**, *3*, 523–542.
(6) Jaiswal, M.; Menon, R. *Polym. Int.* **2006**, *55*, 1371–1384.
(7) Hertel, D.; Scherf, U.; Bassler, H. *Adv. Mater.* **1998**, *10*, 1119–1122.

(8) Sirringhaus, H.; Brown, P. J.; Friend, R. H.; Nielsen, M. M.; Bechgaard, K.; Langeveld-Voss, B. M. W.; Spiering, A. J. H.; Janssen, R. A. J.; Meijer, E. W.; Herwig, P.; de Leeuw, D. M. *Nature* **1999**, *401*, 685–688.
(9) Sirringhaus, H.; Brown, P. J.; Friend, R. H.; Nielsen, M. M.; Bechgaard, K.; Langeveld-Voss, B. M. W.; Spiering, A. J. H.; Janssen, R. A. J.; Meijer, E. W. *Synth. Met.* **2000**, *111*, 129–132.
(10) Sirringhaus, H.; Wilson, R. J.; Friend, R. H.; Inbasekaran, M.; Wu, W.; Woo, E. P.; Grell, M.; Bradley, D. D. C. *Appl. Phys. Lett.* **2000**, *77*, 406–408.
(11) Grozema, F. C.; Savenije, T. J.; Vermeulen, M. J. W.; Siebbeles, L. D. A.; Warman, J. M.; Meisel, A.; Neher, D.; Nothofer, H. G.; Scherf, U. *Adv. Mater.* **2001**, *13*, 1627–1630.
(12) Grozema, F. C.; Hoofman, R.; Candeias, L. P.; de Haas, M. P.; Warman, J. M.; Siebbeles, L. D. A. *J. Phys. Chem. A* **2003**, *107*, 5976–5986.
(13) Grozema, F. C.; Warman, J. M. *Radiat. Phys. Chem.* **2005**, *74*, 234–238.
(14) Candeias, L. P.; Grozema, F. C.; Padmanaban, G.; Ramakrishnan, S.; Siebbeles, L. D. A.; Warman, J. M. *J. Phys. Chem. B* **2003**, *107*, 1554–1558.
(15) Prins, P.; Grozema, F. C.; Galbrecht, F.; Scherf, U.; Siebbeles, L. D. A. *J. Phys. Chem. C* **2007**, *111*, 11104–11112.
(16) Prins, P.; Grozema, F. C.; Schins, J. M.; Patil, S.; Scherf, U.; Siebbeles, L. D. *Phys. Rev. Lett.* **2006**, *96*, 146601.
(17) Chua, L. L.; Zaumseil, J.; Chang, J. F.; Ou, E. C. W.; Ho, P. K. H.; Sirringhaus, H.; Friend, R. H. *Nature* **2005**, *434*, 194–199.

Scheme 1. Synthesis of End-Capped Poly-2,7-(dihexylfluorene)s
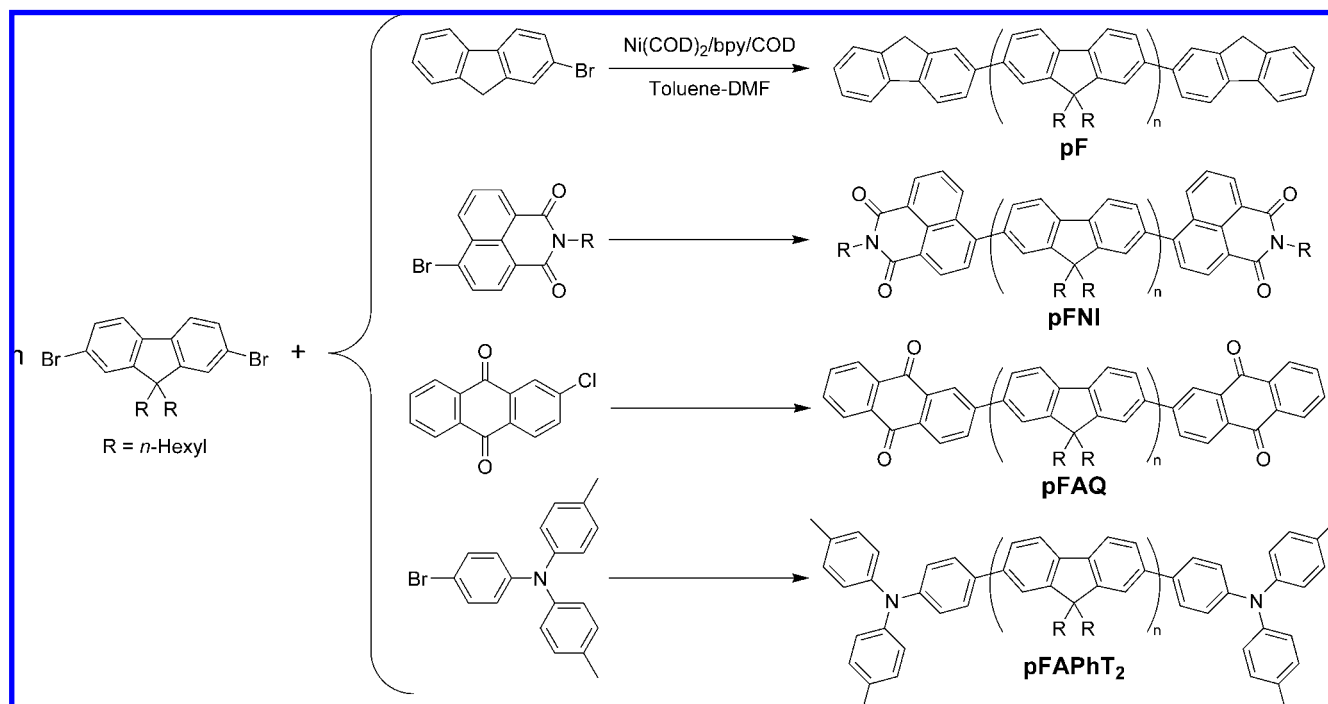
transport might be the weak link for transport in films. But the implications of the Delft results are not yet clear. Especially important is the question: Could those results point to the possibility of highly efficient, "wirelike" charge transport over long distances in photovoltaic or photoemissive devices?

A major challenge to the idea that conjugated polymers can function as semiconducting "molecular wires" capable of transporting charges over long distances comes from information about their conformations. Measurements by light scattering pointed to coiled structures for some polymers expected to be rigid rods in solution.[20,21] Relatively stiff polyphenylene−vinylenes (PPVs) with chain lengths >200 nm were found to exist in solution as compact structures having hydrodynamic radii of ∼10 nm.[22,23] Long PPV polymers "collapse" into coils, globules, toroids, or cylinders[24,25] because of "tetrahedral" and other defects along with the tension of polymer−polymer vs polymer−solvent interactions. How then do we understand high mobilities reported in single strands, including PPVs? The microwave conductivity technique probes mobilities with high frequencies typically near 30 GHz, so the direction of the field changes each ∼15 ps. Clear end effects were reported in a ladder polymer,[16] but for others it is not yet clear whether charges actually move efficiently over large distances. More information is needed.

This article investigates multinanometer transport of charges to traps at the ends of the polymer chains, an approach similar to that used to investigate exciton transport[26] and our earlier examinations of hole[27] and triplet transport.[28] As in the Delft work, the experiments described here utilize the ability of pulse radiolysis to rapidly inject charges into the chains of conjugated polymers. The results reported below appear to be best described in terms of transport over distances of many nanometers within a few nanoseconds and indicate that the technique has promise to make substantial contributions to the broad and complex questions of long distance charge transport.

Experimental Section

Synthesis of End-Capped Poly-2,7-(9,9-dihexylfluorene) (pF−X). The pF−Xs were prepared by polycondensation of 2,7-dibromo-9,9-dihexylfluorene according to the procedure reported by Klaerner and Miller,[29] as shown in Scheme 1. 2-Bromofluorene, *N*-hexyl-4-bromo-1,8-naphthylimide, 2-chloroanthraquinone, or *N*,*N*-bis(4-methylphenyl)-4-bromobenzenamine were used as the end-capping reagents. In a Schlenk tube, bis(1,5-cyclooctadiene) nickel(0) (1.8 mmol), 1,5-cyclooctadiene (1.8 mmol), and 2,2′-bipyridine (1.8 mmol) were dissolved in the mixed solvent of toluene (12 mL) and DMF (12 mL) and heated at 80 °C for 30 min under an argon atmosphere. A toluene solution (8 mL) of 2,7-dibromo-9,9-dihexylfluorene (1.0 mmol) and end-capping reagent (0.1 mmol) was added, and the reaction mixture was heated at 80 °C for 12 h and then poured into an equivolume mixture of concentrated hydrochloric acid, methanol, and acetone. The organic layer was extracted with toluene, washed with brine, and then dried over sodium sulfate. The solvent was removed under reduced

(18) Kline, R. J.; McGehee, M. D.; Kadnikova, E. N.; Liu, J. S.; Frechet, J. M. J. *Adv. Mater.* **2003**, *15*, 1519–1522.

(19) Pinner, D. J.; Friend, R. H.; Tessler, N. *Synth. Met.* **2000**, *111*, 257–261.

(20) Cotts, P. M.; Swager, T. M.; Zhou, Q. *Macromolecules* **1996**, *29*, 7323–7328.

(21) Grell, M.; Bradley, D. D. C.; Long, X.; Chamberlain, T.; Inbasekaran, M.; Woo, E. P.; Soliman, M. *Acta Polym.* **1998**, *49*, 439–444.

(22) Nguyen, T. Q.; Doan, V.; Schwartz, B. J. *J. Chem. Phys.* **1999**, *110*, 4068–4078.

(23) Schwartz, B. J. *Annu. Rev. Phys. Chem.* **2003**, *54*, 141–172.

(24) Wong, K. F.; Skaf, M. S.; Yang, C. Y.; Rossky, P. J.; Bagchi, B.; Hu, D. H.; Yu, J.; Barbara, P. F. *J. Phys. Chem. B* **2001**, *105*, 6103–6107.

(25) Hu, D. H.; Yu, J.; Wong, K.; Bagchi, B.; Rossky, P. J.; Barbara, P. F. *Nature* **2000**, *405*, 1030–1033.

(26) Beljonne, D.; Pourtois, G.; Silva, C.; Hennebicq, E.; Herz, L. M.; Friend, R. H.; Scholes, G. D.; Setayesh, S.; Mullen, K.; Bredas, J. L. *Proc. Natl. Acad. Sci. U.S.A.* **2002**, *99*, 10982–10987.

(27) Funston, A. M.; Silverman, E. E.; Miller, J. R.; Schanze, K. S. *J. Phys. Chem. B* **2004**, *108*, 1544–1555.

(28) Funston, A. M.; Silverman, E. E.; Schanze, K. S.; Miller, J. R. *J. Phys. Chem. B* **2006**, *110*, 17736–17742.

(29) Klaerner, G.; Miller, R. D. *Macromolecules* **1998**, *31*, 2007–2009.

Table 1. Properties of pF Polymers, End-Capping Probabilities, and the Fraction, $F(pF^{\bullet-})$ or $F(pF^{\bullet+})$, of Charges Attached to the Polymer That Result in Long-Lived $pF^{\bullet-}$ or $pF^{\bullet+}$ Ions

| | $M_N{}^a$ | M_W/M_N | $n_{GPC}{}^b$ | $n_{NMR}{}^c$ | $F_{cap}{}^d$ n_{GPC}/n_{NMR} | probability[e] | | | $F(pF^{\bullet-})$ or $F(pF^{\bullet+})^f$ |
						P(2)	P(1)	P(0)	
pF	3280	1.6	9.9	34.2	0.29	0.08	0.42	0.50	
pFNI	12280	2.3	36.9	46.6	0.79	0.63	0.33	0.04	0.23 ± 0.06
pFAQ	4590	2.4	13.8	23.4	0.59	0.35	0.48	0.17	0.18 ± 0.06
pFAPT$_2$	3390	1.4	10.2	26.2	0.39	0.15	0.48	0.37	0.41 ± 0.08

[a] The number-averaged molecular weight by gel permeation chromatography relative to oligofluorene standards. [b] Length in repeat units = M_N/FW; FW is the formula weight of a dihexylfluorene repeat unit. Lengths of the pF chains between the end caps are taken to be smaller by two units. Slightly longer lengths would be obtained if corrections were made for the slightly smaller formula weights of the end caps. [c] Based on NMR integrations (±1%) and assumptions of complete end capping, neglecting polydispersity. [d] Estimated fractions, ±0.1, of the chain ends actually having caps calculated as n_{GPC}/n_{NMR}. [e] Probabilities of having 2, 1, or 0 end caps calculated from F_{cap} assuming that caps are distributed randomly. [f] $F(pF^{\bullet-}) = 0.23$ for pFNI means, for example, that 23% of the electrons attached do not decay rapidly as determined by transient absorption (see below). These long-lived ions react slowly by bimolecular charge transfer and by recombination. The uncertainties reflect both complexities of the fitting and variations in data from run to run.

pressure, and the crude polymer was dissolved in a small amount of chloroform and reprecipitated twice from methanol before Soxhlet extraction with acetone for 3 days to remove low molecular weight oligomers.

The GPC profiles of pF–Xs are shown in Figure S1 in Supporting Information. The number-averaged molecular weight (M_N) and polydispersity (M_W/M_N) were determined on the basis of polystyrene calibration standards (Aldrich). To obtain a more accurate calibration, a series of oligofluorenes with 1–10 fluorene units were synthesized according to the modified procedures reported by Geng et al.[30] (Apparent molecular weights calculated from GPC elution volumes based on polystyrene standards afforded an excellent linear relationship ($R^2 = 0.9985$) to the actual molecular weights.) The averaged polymerization degrees (n_{GPC}) and the number-averaged molecular weights based on these oligofluorene standards are reported in Table 1. Because each end cap adds a length similar to one repeat unit, the end-capped molecules may be described as pF$_{35}$NI, pF$_{12}$AQ, and pF$_8$APT$_2$, two units less than n_{GPC}. We will usually use the shorter abbreviations pFNI, pFAQ, and pFAPT$_2$, except where specific mention of lengths is referred to. The estimated lengths for pF$_{11}$, pF$_{12}$AQ, and pF$_8$APT$_2$ are within or close to the range, $n = 1–10$, given by the oligofluorene standards. For pF$_{35}$NI, we are beyond that range. The extrapolation makes this length less certain by an amount not easily estimated.

The ^{1}H NMR spectra of pF–Xs are shown in Figure S2. The sets of characteristic peaks for end-capping groups were observed in each spectrum together with the large peaks of poly-2,7-(9,9-dihexylfluorene). To estimate the completeness of end capping, the apparent averaged polymerization degrees (n_{NMR}) were calculated on the basis of the molar ratios of monomer units to those of end caps, which were given by the observed ratio of protons on α-carbon of two hexyl groups (4H, 2.1 ppm) of the monomer units to those on 9-positions of terminal unsubstituted fluorenes (2H, 4.02 ppm) in pF, α-carbon of a hexyl group (4.23 ppm) of naphthylimide in pFNI, aromatic ring of anthraquinone (5H, 8.13, 8.38, 8.43, 8.65 ppm) in pFAQ, or methyl groups (6H, 2.33 ppm) of two N-(4-methylphenyl) groups in pFAPT$_2$, respectively. These results are recorded in Table 1. If each chain end had exactly the expected 2.0 caps/molecule, the fraction of capping $F_{cap} = 1.0$, then the degree of polymerization, n_{NMR}, should equal n_{GPC}. This ideal result is not found, implying that end capping is not complete in these molecules. F_{cap} and probabilities of two, one, and zero caps per molecule derived from it are reported in the table. They will be useful in interpretation of charge-transport experiments to be described below. The uncertainty in length from GPC noted above for pF$_{35}$NI makes the capping fractions similarly less certain.

Chemicals. 2-Bromofluorene, 2-chloroanthracene, bis(1,5-cyclooctadiene) nickel(0), 1,5-cyclooctadiene, and 2,2′-bipyridine were used as purchased from Aldrich. A 2,7-dibromo-9,9-dihexylfluorene

monomer was prepared from 2,7-dibromofluorene (Aldrich) according to the procedure as reported previously.[31] N-Hexyl-4-bromo-1,8-naphthylimide was synthesized from 4-bromo-1,8-naphthalic anhydride (Aldrich) treated with n-hexylamine (Aldrich) in anhydrous DMF. ^{1}H NMR: δ_H(CDCl$_3$) 0.89 (t, $J = 7.1$ Hz, 3H), 1.46−1.25 (m, 6H), 1.72 (m, 2H), 4.15 (d, $J = 7.6$ Hz, 1H), 4.17 (d, $J = 7.6$ Hz, 1H), 7.84 (dd, $J = 7.3, 8.5$ Hz, 1H), 8.03 (d, $J = 7.9$ Hz, 1H), 8.40 (d, $J = 7.9$ Hz, 1H), 8.55 (dd, $J = 1.1, 8.5$ Hz, 1H), 8.65 (dd, $J = 1.1, 7.3$ Hz, 1H). N-Hexyl-1,8-naphthylimide (hex-NI) was prepared from 1,8-naphthalic anhydride (Aldrich) according to the same procedure. ^{1}H NMR: δ_H(CDCl$_3$) 0.89 (t, $J = 6.7$ Hz, 3H), 1.49−1.24 (m, 6H), 1.73 (m, 2H), 4.17 (d, $J = 7.6$ Hz, 1H), 4.19 (d, $J = 7.6$ Hz, 1H), 7.75 (dd, $J = 7.2, 7.9$ Hz, 2H), 8.20 (d, $J = 7.9$ Hz, 2H), 8.60 (d, $J = 7.2$ Hz, 2H). N,N-Bis(4-methylphenyl)-4-bromobenzenamine was prepared according to the procedure reported by Goodbrand and Hu[32] ^{1}H NMR: δ_H(CDCl$_3$) 2.30 (s, 6H), 6.88 (m, 2H), 6.96 (m, 4H), 7.06 (m, 4H), 7.26 (m, 2H).

Pulse Radiolysis. This work was carried out at the Brookhaven National Laboratory Laser-Electron Accelerator Facility (LEAF). The LEAF facility and the methods used are described elsewhere,[33−35] as are application to conjugated polymers.[27,31] Briefly, the electron pulse (≤50 ps duration) was focused into a quartz cell with an optical path length of 20 or 5 mm containing the solution of interest under argon or vacuum in either tetrahydrofuran (THF) or 1,2-dichloroethane (DCE). The monitoring light source was a pulsed xenon arc lamp. Wavelengths were selected using either 40- or 10-nm band-pass interference filters. Transient absorption signals were detected with either silicon (EG&G FND-100Q, ≤1000 nm) or InGaAs (GPD Optoelectronics GAP-500 L, ≥1100 nm) photodiodes or a biplanar phototube (Hamamatsu R1328U-03, ≤650 nm) and digitized with a Tektronix TDS-680B or TDS-694C oscilloscope. While most measurements have 2−4-ns time resolution, 125-ps system rise time is attainable in the visible using the biplanar phototube, the 694 scope, and short path cells.

Fast electrons pass through the sample cell, creating ionization that primarily results in reactive solvated electrons ($e_s{}^-$) in THF or radical cations (DCE$^{\bullet+}$) in DCE. These electrons or "holes" are thermalized within a few picoseconds and attach to the polymers in bimolecular charge-transfer reactions. Counterions fragment to

(30) Geng, Y. H.; Trajkovska, A.; Katsis, D.; Ou, J. J.; Culligan, S. W.; Chen, S. H. *J. Am. Chem. Soc.* **2002**, *124*, 8337–8347.

(31) Takeda, N.; Asaoka, S.; Miller, J. R. *J. Am. Chem. Soc.* **2006**, *128*, 16073–16082.

(32) Goodbrand, H. B.; Hu, N.-X. *J. Org. Chem.* **1999**, *64*, 670–674.
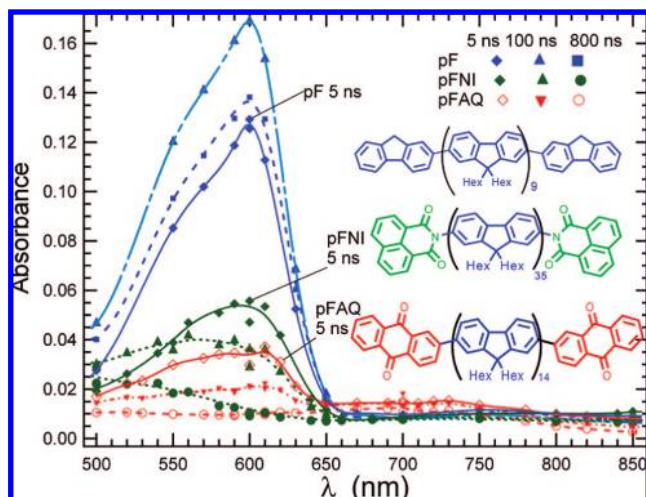
(33) Wishart, J. F. In *Radiation Chemistry: Present Status and Future Trends*; Jonah, C. D., Rao, B. S. M., Eds.; Elsevier Science: Amsterdam, 2001; Vol. 87, pp 21−35.

(34) Wishart, J. F.; Cook, A. R.; Miller, J. R. *Rev. Sci. Instrum.* **2004**, *75*, 4359–4366.

(35) Miller, J. R.; Penfield, K.; Johnson, M.; Closs, G.; Green, N. In *Photochemistry and Radiation Chemistry. Complementary Methods for the Study of Electron Transfer*; Wishart, J. F., Nocera, D. G., Eds.; American Chemical Society: Washington, DC, 1998; Vol. 254, pp 161−176.
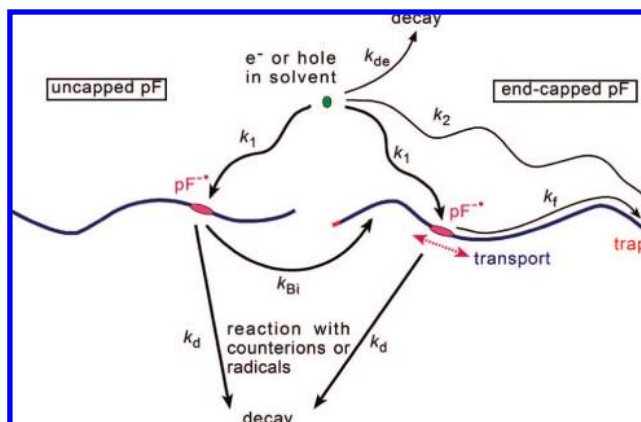
ARTICLES

Figure 1. Transient absorption spectra of pF, pFNI, and pFAQ at 9.7, 9.9, and 9.3 mM (repeat unit concentration) in THF in 2-cm cells measured with the FND-100 detector (2-ns rise time). Each spectrum is shown at 5, 100, and 800 ns.
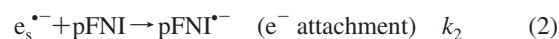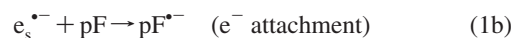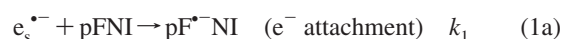

Figure 2. Charge attachment to a pF chain with rate k_1 followed by rapid transport to and trapping by an end cap with rate k_f (right). Direct charge attachment to end caps occurs with rate k_2. Polyfluorene molecules with no end caps (left) also capture the charge with rate k_1 and transfer it to end-capped pF with bimolecular rate constant k_{Bi}. Concomitantly, charge (e^- or hole) in solvent and $pF^{\bullet-}$ reacts with counterions or radicals and decays with rate k_{de} and k_d, respectively.

solvated protons in THF or Cl^- in DCE. The transmission/time data were analyzed, and reaction rate constants were determined in scheme that accounts for geminate and homogeneous recombination with the counterions. A kinetic model was fit to the data using nonlinear least-squares fitting in Igor Pro software (Wavemetrics). Where not stated, uncertainties are 15%. Molar extinction coefficients of the radical ions were obtained by comparison to measurements under the same conditions with ions having known values. Reference extinction coefficients (M^{-1} cm^{-1}) for anions were $\varepsilon(\text{benzophenone}^{\bullet-}, 754 \text{ nm}) = 8.5 \times 10^3$ [36] and $\varepsilon(e_s^-, 2120$ nm$) = 4.0 \times 10^4$,[37] and $\varepsilon(\text{tritolylamine}^{\bullet+}, 670 \text{ nm}) = 2.75 \times 10^4$ [38] for cations.

Results and Discussion

Attachment of electrons to polyfluorene in THF creates anions ($pF^{\bullet-}$) having an intense, $\varepsilon = 7 \times 10^4$ M^{-1} cm^{-1} absorption band at 600 nm,[31] and a near IR band peaking at 2500 nm.[31] The excess electron in $pF^{\bullet-}$ was found to be delocalized over 4.5 repeat units[31] and will be referred to as a "polaron", consistent with reports on charges in other conjugated polymers.[31,39,40] The terms radical anion, polaron, and $pF^{\bullet-}$ will sometimes be used interchangeably. Figure 1 shows transient absorption spectra in the visible region for solutions of pF, pFNI, and pFAQ; more complete spectra are available in Figures S3 and S4. In the solution of pF, the absorbance grew over several nanoseconds to exceed 200 mA. Its kinetics were described previously.[31] The present results also find a nondiffusional contribution that will be described briefly below.

Because attachment of solvated electrons to pF chains is diffusion-controlled,[31] the electrons are assumed to react statistically along the length of the pFAQ and pFNI molecules. On this basis, most electrons (~86% in pFAQ and 95% in pFNI) are expected to attach to the long (10 and 30 nm, respectively) pF chains to form $pF^{\bullet-}$. Therefore, if charge transport along

(36) Pedersen, S. U.; Christensen, T. B.; Thomasen, T.; Daasbjerg, K. *J. Electroanal. Chem.* **1998**, *454*, 123–143.

(37) Dorfman, L. M.; Jou, F. Y.; Wageman, R. *Ber. Bunsen-Ges. Phys. Chem.* **1971**, *75*, 681–685.

(38) Pedersen, L.; Pedersen, S. U. University of Aarhus, Private communication, 2005.

(39) Furukawa, Y. *J. Phys. Chem.* **1996**, *100*, 15644–15653.

(40) Wohlgenannt, M.; Jiang, X. M.; Vardeny, Z. V. *Phys. Rev. B* **2004**, *69*, 241204.

the pF chains is slow, initial absorptions in pFNI and pFAQ are expected to be ~90% of those for pF without traps. Instead, the data in Figure 1 show that at $t = 5$ ns only a fraction of the electrons attached to pFAQ and pFNI are observed as $pF^{\bullet-}$ in the chains. Data in Figure 1 thus point to the interpretation that electron attachment is followed by rapid transport to and trapping by the electron-accepting AQ and NI end cap groups as depicted in Figure 2. In Figure 1, a small fraction of the $pF^{\bullet-}$ spectrum remains at 100 ns for both pFAQ and pFNI. This is attributed to the presence of chains having no AQ or NI end caps as anticipated from capping estimates in Table 1.

Figure 2 also includes reactions that cause the decay of e^- (or holes) and $pF^{\bullet-}$ ions by reactions with counterions in the solvent and bimolecular reactions of $pF^{\bullet-}$ with AQ or NI groups on other chains.

The reactions, depicted in Figure 2, are included in kinetic scheme of charge capture, transport, and trapping in polymer molecules with end caps. Taking pFNI as an example, reactions (i) and (ii) are chemistry of the solvent, THF, abbreviated as RH. They are fast so that within a few picoseconds the ionizing electron pulse produces thermalized, solvated electrons ($e_s^{\bullet-}$), while reaction (ii) has converted the solvent hole into solvated protons (RH_2^+) and radicals, neither of which reacts with pFNI or similar molecules. The same scheme was utilized for hole transport in DCE, but a different fragmentation reaction involving the electron replaces (ii), resulting in only reactive solvent holes.

$$RH \rightarrow RH^{\bullet+} + e_s^{\bullet-} \quad \text{(ionization)} \tag{i}$$

$$RH^{\bullet+} + RH \rightarrow R^{\bullet} + RH_2^+ \quad \text{(proton transfer)} \tag{ii}$$

$$e_s^{\bullet-} + pFNI \rightarrow pF^{\bullet-}NI \quad (e^- \text{ attachment}) \quad k_1 \tag{1a}$$

$$e_s^{\bullet-} + pF \rightarrow pF^{\bullet-} \quad (e^- \text{ attachment}) \tag{1b}$$

$$e_s^{\bullet-} + pFNI \rightarrow pFNI^{\bullet-} \quad (e^- \text{ attachment}) \quad k_2 \tag{2}$$

$$pF^{\bullet-}NI, pFNI^{\bullet-} + RH_2^+, \ R^{\bullet} \rightarrow products \quad k_d \tag{3}$$

$$e_s^{\bullet-} + RH_2^+, R^{\bullet} \rightarrow products \quad k_{de} \tag{4}$$

$$pF^{\bullet-}NI \rightarrow pFNI^{\bullet-} \quad (\text{intramolecular CT}) \quad k_f \tag{5}$$

$$pF^{\bullet-} + pFNI \rightarrow pF + pFNI^{\bullet-} \quad k_{Bi} \quad (6)$$

Because decomposition of THF cations (reaction ii) occurs in 0.5 ps,[41] ionization of THF yields electrons and anions of solutes such as pF with almost no positive ions. The very small amounts of cations and excited states formed are neglected.

The following sections of this article will examine the interpretation that fast charge transport occurs in end-capped molecules and evaluate the rates within the scheme of reactions 1a–6. More information about the fitting procedure is described below. First, we report the spectra observed and determine their extinction coefficients. The spectra will establish that two dominant species are formed upon charge attachment: $pF^{\bullet-}$ polarons and end cap trapped anions; in the case of $pFAPT_2$ in DCE the two species are $pF^{\bullet+}$ polarons and end cap cations. All three end cap ions will be shown to possess remarkable charge-transfer bands. Also described below will be measurements with high, near-saturation concentrations of pFAQ and pFNI and a faster detector to resolve the charge transport to the end caps. First, it is useful to describe the spectra formed by charge attachment.

Spectra of Charges Attached to End Caps. Figure 3 shows spectra at 1.0 μs when the bands of $pF^{\bullet-}$ are absent and new bands due to $pFNI^{\bullet-}$ and $pFAQ^{\bullet-}$ are evident, due to charges trapped on the end caps. At early times, the known spectrum of $pF^{\bullet-}$ [31] is seen at reduced intensities (Figures 1 and S3 and S4).

Figure 4 shows the spectrum obtained when holes are attached to polyfluorene having APT_2 hole traps in DCE. As with the polymers containing electron traps, the spectrum[31] of $pF^{\bullet+}$ is absent at long time (5 μs), being replaced by a new spectrum due to charges trapped on the end caps. As for the anions, the spectrum of $pF^{\bullet+}$ is seen with reduced intensity at early times (Figure S5). The spectrum of the end cap trapped hole is distinctly different from that of tritolylamine$^{\bullet+}$ (TTA$^{\bullet+}$), a model for the end cap group.

Charge-Transfer Bands. Figures 3 and 4 show that electrons attached to pFNI or pFAQ and holes attached to $pFAPT_2$ produce new optical absorption bands. Observations described below will establish that these are charge-transfer bands of electrons or holes trapped on the end caps. The new bands of $pFNI^{\bullet-}$ or $pFAQ^{\bullet-}$ bear no resemblance to the spectra of $pF^{\bullet-}$ ions. Similarly, the absorption of $pFAPT_2^{\bullet+}$ is unlike the spectrum of $pF^{\bullet+}$. Neither do these new bands resemble spectra of the radical ions of the end cap molecules, shown for comparison in each graph; these are entirely new species. With the exception of one report from this laboratory,[27] spectra of these interesting species have not been reported. The finding that the spectra appear entirely new is not surprising because the end caps are conjugated with the polymer chains in all three cases. The new bands are broad, without sharp vibrational features, as is typical for charge-transfer bands. If these are charge-transfer bands that remove the charge from the trap and reinject it into the polymer chain, then their energies should correlate with differences between corresponding redox potentials; this is tested below.

Table 2 reports the maxima and estimated origins of the largest spectral features, with bands peaking at 1.21 eV in $pFNI^{\bullet-}$, 1.7 (and 1.84) eV in $pFAQ^{\bullet-}$, and 1.03 eV in $pFAPT_2^{\bullet+}$, together with redox potentials determined by cyclic voltammetry for the end-capped polymers. The spectra of these bands are fit

(41) Martini, I. B.; Barthel, E. R.; Schwartz, B. J. *J. Chem. Phys.* **2000**, *113*, 11245–11257.
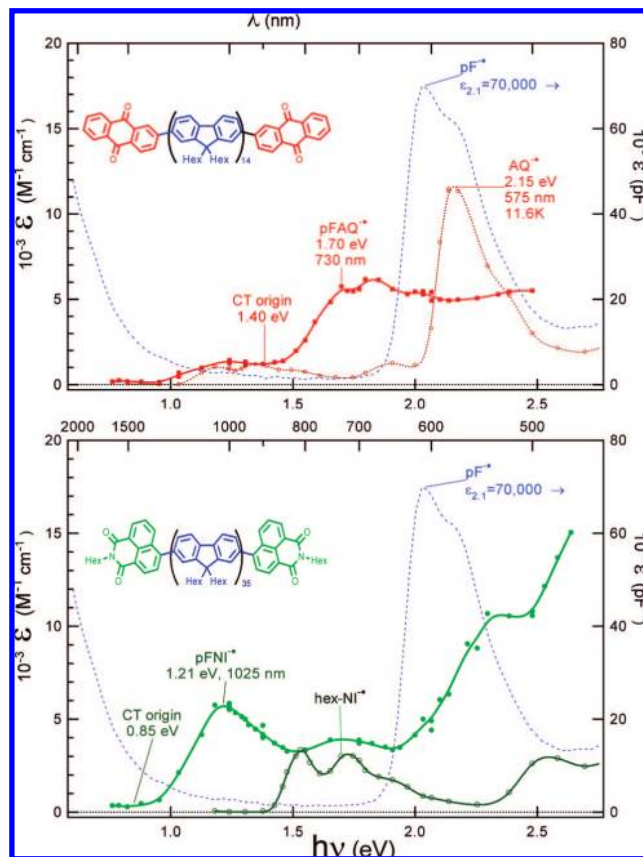
Figure 3. Transient absorption spectra of $pFAQ^{\bullet-}$ and $pFNI^{\bullet-}$ in THF at 1.0 μs. For comparison, spectra of $pF^{\bullet-}$, $AQ^{\bullet-}$, and $hexNI^{\bullet-}$ are also shown; the more intense spectrum of $pF^{\bullet-}$ formed in a solution of pF is shown at reduced scale (right axis).
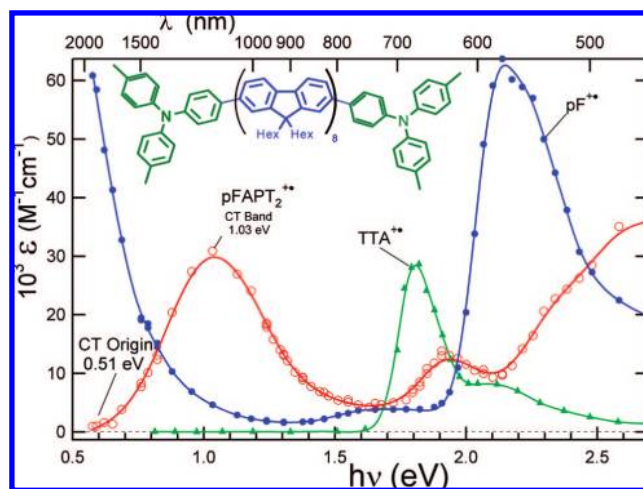
Figure 4. Transient absorption spectrum of holes attached to 10 mM $pFAPT_2$ at 5 μs in DCE. For comparison, spectra of $pF^{\bullet+}$ and TTA$^{\bullet+}$ are also shown.

well with a charge-transfer expression (see footnote [c]), to determine their origins as well as maxima. A plot of the origins of the bands vs the redox potential of the capped compound relative to that of uncapped pF is linear with a slope of 1.0 (Figure 5) and intercepts the origin. A plot of the maxima is not as linear, probably reflecting different amounts of structural change (reorganization energies) associated with removing charges from the different end caps. Molecular orbital calculations on ions of F_5NI, F_5AQ, and F_5APT also identify these
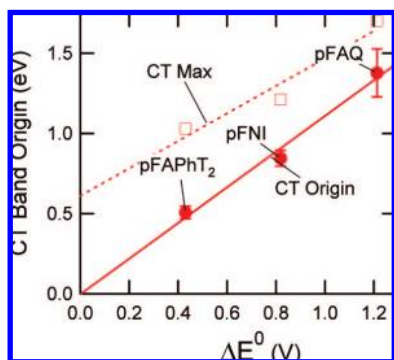
Table 2. Redox Potentials and Charge Transfer Bands

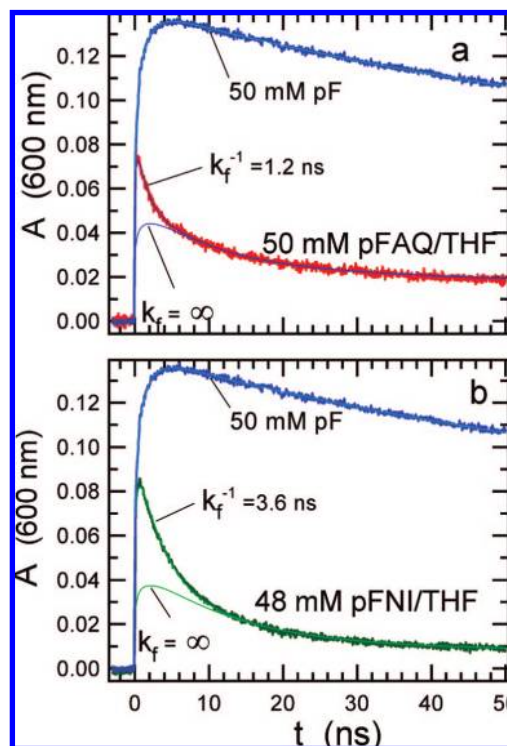|	E^0 (V)[a] vs Fc$^{+/0}$	$\Delta(E^0)$[b] (eV)	CT origin (eV)[c]	CT E_{max} (eV)	λ (eV)[d]
pF$^{0/-}$	−2.65				
pFNI$^{0/-}$	−1.831	0.819	0.85	1.21	0.40
pFAQ$^{0/-}$	−1.437	1.213	1.40	1.7	0.54
hexNI	−1.88				
AQ	−1.34				
pF$^{+/0}$	0.66				
pFAPT$_2^{+/0}$	0.24[e]	0.42	0.51	1.03	0.57
TTA	0.23[f]				

[a] From cyclic voltammetry in THF/0.1 M Bu$_4$NBF$_4$ (Figure S6). Waves for reduction of pF chains were too broad to determine potentials, which were determined instead from charge-transfer equilibria,[31] with compounds that do exhibit reversible potentials vs Fc$^{+/0}$ internal standard. [b] The difference between the redox potential for pF and the end-capped pF. [c] Origin of the charge-transfer band estimated by fitting to an expression[42] having a solvent reorganization energy (Macrus theory) and one molecular vibration. [d] Reorganization energies from fits to the charge-transfer spectra that include low frequency, principally solvent, and high frequency molecular modes. [e] From the potential E^0(TTA$^{+/0}$), and the 0.01 V difference between E^0(TTA$^{+/0}$) and E^0(pFAPT$_2^{+/0}$) reported by Miteva et al. For pFAPT$_2^{+/0}$, Miteva et al. reported E^0 = 0.68 V vs Ag/AgCl.[43] [f] Determined from the potential for triphenylamine, E^0(TPA$^{+/0}$) = 0.40[44] vs Fc$^{+/0}$ and the 0.17 V difference[45] between TPA and TTA. Miteva et al. reported E^0(TTA$^{+/0}$) = 0.67 V vs Ag/AgCl.[43]

Figure 5. Energies of charge-transfer band origins plotted as a function of the redox potentials of the end-capped molecules relative to that of pF (Table 2). The maxima of the bands are also shown.

transitions as including substantial fractions of charge-transfer configurations.

Charge Transport to End Caps. Figure 6 shows transient absorption as a function of time at ∼50 mM (in repeat units) of pF, pFAQ, and pFNI in THF. The high concentrations capture electrons rapidly enough to compete with transport with rate k_f, of the pF$^{•-}$ polarons to the AQ or NI end caps. Kinetic fits to the data shown in Figure 6 obtain intramolecular "rate constants" $k_f = 8.5 \times 10^8$ (pFAQ) and 2.8×10^8 s^{-1} (pFNI). Fractions F(pF$^{•-}$), reported in Table 1, do not decay with k_f, reacting much more slowly. Similar data (Figure S7) on pFAPT$_2$ in DCE do not resolve the hole transport, determining the lower limit, $k_f > 1 \times 10^8$ s^{-1}. For pFNI and pFAQ, two additional sets of data are shown in Supporting Information at lower concentrations. Data at 15 mM repeat unit concentrations of

(42) Penfield, K. W.; Miller, J. R.; Paddonrow, M. N.; Cotsaris, E.; Oliver, A. M.; Hush, N. S. *J. Am. Chem. Soc.* **1987**, *109*, 5061–5065.
(43) Miteva, T.; Meisel, A.; Knoll, W.; Nothofer, H. G.; Scherf, U.; Muller, D. C.; Meerholz, K.; Yasuda, A.; Neher, D. *Adv. Mater.* **2001**, *13*, 565–570.
(44) Luo, H. X.; Fujitsuka, M.; Araki, Y.; Ito, O.; Padmawar, P.; Chiang, L. Y. *J. Phys. Chem. B* **2003**, *107*, 9312–9318.
(45) Seo, E. T.; Nelson, R. F.; Fritsch, J. M.; Marcoux, L. S.; Leedy, D. W.; Adams, R. N. *J. Am. Chem. Soc.* **1966**, *88*, 3498–3503.

Figure 6. Transient absorption at 600 nm of pF, pFAQ (a), and pFNI (b) at ∼50 mM (repeat units) in THF. Kinetic fits giving intramolecular rate constants, k_f, bimolecular rate constants, k_{Bi}, and other parameters for electron attachment and geminate and homogeneous decay almost coincide with the data. Fit curves are also shown with all parameters fixed and k_f set to infinity. The biplanar phototube and 5 mm cells gave 125-ps rise time.

pFNI and pFAQ (Figure S8) are similar to that in Figure 6, but the fits yield lower rates of intramolecular transport, $k_f = 3.0 \times 10^8$ (pFAQ) and 1.3×10^8 s^{-1} (pFNI). At 2 mM (Figure S9), the results indicate that a similar fraction of the pF$^{•-}$ disappears by a fast process, but because of slow electron attachment the data determine that k_f is fast ($\gg 10^8$). The fitting procedure is discussed below.

Determination of Charge Transport. The fitting procedure performs nonlinear, least-squares fits for reactions 1−6. It is illustrated in Figure 2 and, with more detail, in Figure S10. The growth of anions must take into account of the decay of electrons, so the procedure begins with a fit to the solvent alone to find kinetics of the solvated electrons. Their nonexponential electron decay is represented with two geminate and one homogeneous fraction having different values of k_{de}. This sum of exponentials enabled use of analytic solutions to the entire system of differential equations for reactions 1a−6. Those parameters describing the electron were then fixed to fit pF without end caps. Because electrons or holes are attached to the capped pF molecules in diffusional, bimolecular processes, conclusions about transport are intimately coupled to the kinetics of charge attachment to molecules such as pFNI and pFAQ.

Takeda et al.[31] reported $k(e_s^- + pF_{10}) = 2.6 \times 10^{10}$ M^{-1} s^{-1} (per monomer) or 2.6×10^{11} M^{-1} s^{-1} (per polymer). For 50 mM monomer, this gives a capture rate of 1.3×10^9 s^{-1} or ∼0.8 ns. But the charge capture could not be described by ordinary pseudo-first-order kinetics. Departures from simple kinetics are expected from transient terms in the equations describing diffusion-controlled equations first described by

Smoluchowski[46] and later expanded upon.[12,47−49] Such theories have been used to describe transient effects in electron or hole attachment to long objects such as a polymers previously.[12,27,31]

In the present work, the attachment process was treated as the principal exponential $k_{att}c$, noted above where c is polymer concentration, and a smaller fraction of a second, faster rate component simulating the transient term. Transient contributions to diffusion-controlled reactions of small, spherical reactants contain a $t^{-1/2}$ term and are therefore not exponential in time. The use of two exponentials here obtained satisfactory descriptions of pF$^{\bullet-}$ growth while still allowing use of the analytic solutions. Successful description of the data for pF$^{\bullet-}$ growth was obtained (upper, pF, curves in Figures 6 and S9), but only with the additional inclusion of a substantial component of "prompt" electron capture. Prompt capture refers to electron attachment that occurs before diffusion of the solvated electrons, perhaps before thermalization, similar to "dry electron" capture that was first discussed decades ago.[50−54] The fraction of electrons captured promptly was $(1 - e^{-qc})$; q was close to 100 M^{-1} (polymer concentration) for pF and pFAQ and was three times larger for the longer polymer, pFNI. After formation, the pF$^{\bullet-}$ ions decayed by 21% in the 50-ns window of Figure 6 because of recombination (reaction 3). This decay was described with the two geminate and one homogeneous decay, as for the electrons. Once these parameters were determined in the fit to pF, they were fixed; the same decay was assumed to occur for the end-capped ions.

Next, the traces for pFAQ and pFNI were fit to obtain k_f and the bimolecular charge transfer rate constant, k_{Bi}. Rates of electron attachment to pFAQ were similar to those for pF; for pFNI they were larger because their lengths were different from that of pF. Extinction coefficients for the final products, in which the charges reside on the AQ or NI groups, were from long time data (Figure 3). The rate constants, k_f, that give best fits for intramolecular transport in pFAQ$^{\bullet-}$ and pFNI$^{\bullet-}$ are ~2.5 times larger in the 50 mM solutions (Figure 6) than those in 15 mM solutions (Figure S8). It might therefore be tempting to assume that k_f is small and attribute the fast components to bimolecular reactions. Such an explanation is untenable. For the 15 mM solutions, it would require that ~70% of the anions formed react with bimolecular rate constants of 3×10^{11} M^{-1} s^{-1}. Such high rates are implausible even for smaller molecules having larger diffusion coefficients. Such a hypothesis would provide no explanation for the 2 mM data (Figure S9), which show much slower decay due to the bimolecular reactions. In the 2 mM data, k_f is not directly observed; we only see that most pF$^{\bullet-}$ ions are absent in the end-capped molecules.

The results are better understood if the fast components, observable at high concentrations, are due to intramolecular transport, k_f, which is uncertain by a factor of 2. A principal reason for the uncertainty is our treatment of k_f as a single exponential process although pFAQ and pFNI molecules have

distributions of lengths and some have only one end cap; both of these factors should lead to a distribution of rates. A more complex description has not been implemented. At present, we suspect it would not yield unique results. To be more meaningful, it would require better knowledge of other parameters that are needed in the kinetic model. Incorrect values of these parameters in the fit could make up for shortcomings in the single-exponential description of the transport and trapping process might bias the result.

Principal among these is uncertainty from the bimolecular transfer. This rate, k_{Bi}, is the principal reason for decay of molecules not having end caps and also contributes to those with caps. The fits determine k_{Bi}, treating the decay it causes as a single exponential. But the rate constants may have transient terms such as those found for electron attachment. Little is known about such bimolecular reactions of long molecules. A related factor is the fraction of molecules in which pF$^{\bullet-}$ ions react only with end caps on other molecules and the slower ion recombination. This fraction, $F(pF^{\bullet-})$, as determined by the transient absorption data, can be compared with estimates based on GPC/NMR (Table 1) of the fraction of molecules having no end caps. Table 1 notes good agreement is found for pFAQ and pFAPT$_2$, but not for pFNI. Only 4% of pFNI was predicted to be completely without end caps, but $F(pF^{\bullet-}) = 0.23$ was found to react by the slow, bimolecular route. This lack of agreement could signal that a fraction, ~19%, of electrons are blocked by defects. Alternatively, the fraction of end capping in pF$_{35}$NI might be lower than estimated, given the uncertainty noted above in the length determined by GPC. In the future, we hope that new synthetic methods will enable more complete end-capping to surmount this difficulty.

Incomplete knowledge of charge attachment is another source of uncertainty in determination of k_f. The time resolution of the present experiments is not adequate to fully distinguish the fast components of nonexponential diffusional capture from prompt capture, which, in turn, affects determination of the early parts of pF$^{\bullet-}$ decay. An additional factor is incomplete determination of the fraction of charges that attach directly to the end caps, rate process (2) in the scheme. This fraction was also determined, but not with high accuracy. In the next few years, we hope to find new molecules and methods to improve upon the rough, single-exponential description of k_f, understood as an average transport rate having a factor of 2 uncertainty.

A conclusion of the present work then is that end capping is not complete in these molecules. Incomplete end capping has been reported and well documented by the McCullough group[55−57] and may be typical in synthesis of end-capped polymers. Its effects were recognized in a previous study by some of us,[28] but its effects were not recognized in our earlier work.[27] It is not known whether it might be present in others.[26]

An important result noted in Table 3 is that ~70% of the charges attached to pFNI and pFAQ were observed to be in the pF chains and to transport to the end caps in rate processes described approximately with a single transport time, τ, for each, which can be used to estimate mobilities.

Appearance on End Caps. The principal absorption bands of the charges trapped on the end caps diagnose the presence of electrons or holes on the end caps. Their transient absorptions

(46) Smoluchowski, M. *Z. Phys.* **1916**, *17*, 557–571.
(47) Noyes, R. M. *Prog. React. Kinet.* **1961**, *1*, 129–160.
(48) Traytak, S. D. *Chem. Phys. Lett.* **1992**, *197*, 247–254.
(49) Traytak, S. D. *Chem. Phys. Lett.* **1994**, *227*, 180–186.
(50) Wolff, R. K.; Bronskill, M. J.; Hunt, J. W. *J. Chem. Phys.* **1970**, *53*, 4211–4215.
(51) Lam, K. Y.; Hunt, J. W. *Int. J. Radiat. Phys. Chem.* **1975**, *7*, 317–338.
(52) Jonah, C. D.; Miller, J. R.; Matheson, M. S. *J. Phys. Chem.* **1977**, *81*, 1618–1622.
(53) Razem, D.; Hamill, W. H. *J. Phys. Chem.* **1978**, *82*, 1347–1351.
(54) Lewis, M. A.; Jonah, C. D. *J. Phys. Chem.* **1986**, *90*, 5367–5372.

(55) Liu, J. S.; McCullough, R. D. *Macromolecules* **2002**, *35*, 9882–9889.
(56) Jeffries-El, M.; Sauve, G.; McCullough, R. D. *Macromolecules* **2005**, *38*, 10346–10352.
(57) Liu, J. S.; Loewe, R. S.; McCullough, R. D. *Macromolecules* **1999**, *32*, 5777–5785.

Table 3. Rates of Charge Attachment and Charge Transport to End Caps with Mobilities Estimated for Complete Capping

	$k_{att}{}^a$ M^{-1} s^{-1}	τ^b ns	$F(\tau)^c$	$k_{Bi}{}^d$ M^{-1} s^{-1}	ν^{-1} ps^e	μ^f cm^2/Vs
pFAQ	1.1×10^{11}	2.0	0.67	4.1×10^{10}	27	5.4×10^{-3}
pFNI	1.9×10^{11}	5.3	0.72	5.3×10^{10}	87	1.6×10^{-3}
pFAPT$_2$	1.8×10^{10}	<10		6.3×10^{9}	<700	$>2 \times 10^{-4}$

^{a} Electron or hole attachment rate constant per concentration of polymer molecules. ^{b} Time for transport to and capture by the electron or hole accepting end cap. This is an average of reaction times from fits to data in Figures 6 and S8 giving for pFAQ k_f = 8.5 or 3.0 × 10^8 and for pFNI 2.8 and 1.3 × 10^8 s^{-1}. It is uncertain by a factor of 2 (see text). Direct capture at the end caps accounted for. ^{c} Fraction (±0.1) of charges observed to transfer to the end caps with time constant τ. $F(\tau)$ is less than 1.0 because of direct capture by the end caps, 15 ± 8% of the charges attached to pFAQ and 5 ± 5% (pFNI), and the fractions having no end caps (Table 1). ^{d} Bimolecular rate constant for transfer of electrons or holes from uncapped pF molecules to capped ones. For pFAQ and pFNI, the apparent rate constants are for 50 mM (repeat units) concentrations and decrease with decreasing concentration (see text). The rate constants were calculated on the basis of concentrations of polymer molecules having at least one cap. Uncertain by ±20%. ^{e} Average time for a hop moving the charge by one repeat unit from eq 2. Uncertain by a factor of 2. This estimate does not include effects of singly capped chains. The actual hop rates could be faster. ^{f} Mobility from eq 3. Uncertain by a factor of 2.

do not give high time resolution and accuracy in determination of charge transport because those bands lie in the deep red or near-infrared where the fastest detector is not useful. pFNI$^{\bullet-}$ and pFAQ$^{\bullet-}$ have extinction coefficients only moderately larger than those of pF$^{\bullet-}$. Figures S11 and S12 show that electrons attached to pFNI$^{\bullet-}$ and pFAQ$^{\bullet-}$ appear rapidly on the NI or AQ end caps. Similarly, the 1200-nm trace in Figure S7 shows the appearance of positive charge on the end cap of pFAPT$_2$. While fits were not performed on the growths of these bands, they appear to be consistent with the estimates of k_f discussed above.

Charge Transfer and Estimates of Mobility. The results of the experiments described here can be compared with solutions to the differential equations for one-dimensional random walk to traps. Under the assumption that once an electron or hole reaches an AQ, NI, or APT$_2$ end cap, charge transfer to the end cap is fast, the rate is limited by transport, and we can apply known results for one-dimensional diffusion.[58−60] The solutions in the form of a series have been applied to diffusion in nonconjugated polymers containing traps.[59,60] For an initial uniform distribution of charges on chains of length l units having traps at both ends, their expression relates the surviving fraction $P(t)$ to the frequency ν for jumps between adjacent units:

$$P(t) = \sum_{n=0}^{\infty} \frac{1}{(2n+1)^2} \exp\left[-\frac{\pi^2}{2}\frac{1}{(2n+1)^2}\frac{\nu t}{l^2}\right] \bigg/ \sum_{n=0}^{\infty} \frac{1}{(2n+1)^2} \tag{7}$$

The use of a uniform distribution corresponds to the reasonable assumption that electron or hole capture is equally likely at any position along a chain. Curves giving the surviving fraction of charges from eq 7 for chains of length from 12 and 35, corresponding to the average lengths of pF$_{12}$AQ and pF$_{35}$NI, are shown in Figure S13; Figure S14 shows the hopping process. Each term in the series contains an exponential of t/l^2. Because l is larger by almost a factor of 3 for pF$_{35}$NI relative to that for pF$_{12}$AQ, eq 7 predicts an average time τ for transport to the end caps to be longer by a factor of 8.5 in pF$_{35}$NI. Instead, the data in Figure 3 indicate that k_f(pF$_{12}$AQ)/k_f(pF$_{35}$NI) $\cong$ 2.7, suggesting a relationship closer to linear in the length. This disparity could indicate that the transport mechanism is not exactly as described in eq 7, but the disparity is not definitely established by the present data given the factor of 2 uncertainties

in each of the rates. Equation 7 also assumes that both ends of each chain have electron-trapping end caps, but measurements summarized in Table 1 indicate that more chains have only one end cap than two. If the observed τ were interpreted in terms of singly capped chains, the mobility would be four times larger. This might account for the disparity, but our knowledge of the capping is not sufficient for a detailed analysis. Instead, eq 7 is utilized to provide rough estimates of average hopping times and motilities, recognizing that the transport would be faster if the effects of incomplete capping could be included in a fully quantitative way.

On the basis of complete capping, eq 7 gives average jump times from one repeat unit to the next of ν^{-1} = 87 and 27 ps for pF$_{12}$AQ and pF$_{35}$NI as reported in Table 3 along with the corresponding mobilities utilizing eq 8.[61]

$$\mu = \frac{\lambda^2 e \nu}{2 k_B T} \tag{8}$$

In eqs 7 and 8, hops of one repeat unit (λ in eq 8) are assumed; ν^{-1} is the average hopping time. The mean of mobilities determined for pF$_{12}$AQ and pF$_{35}$NI yield μ(pF$^{\bullet-}$) = 3.5 × 10^{-3} cm^2/V with an uncertainty of a factor of 2. Mobilities two decades higher in trans-decalin were reported by Grozema et al.: μ(pF$^{\bullet-}$), μ(pF$^{\bullet+}$) > 0.5 cm^2/V[13] and μ(pF$^{\bullet+}$) = 0.74 cm^2/V in benzene[62] by microwave conductivity. Possible reasons for the difference include the larger polarity of the THF solvent used here compared to that of the nonpolar solvents used in microwave conductivity experiments. The necessity for the polaron to move with a cloud of partly oriented permanent solvent dipoles might considerably slow its motion in the present work. Another possibility is related to the assumption that mobility is independent of length. That assumption is not yet verified and is indeed one of the motivations for the present experiments. It is conceivable the polarons in conjugated polymers such as pF move very rapidly within favorable, nearly planar, regions, but encounter barriers to moving out of those regions. While there could be many sources for such barriers, one might be the need for simple conformational relaxations to create more favorable dihedral angles. In the presence of such barriers, the mobilities from different experiments would be averages of different types. Over distances that require passing through barriers, average mobilities would be small. These might be termed long-distance mobilities. While Prins et al.[16] reported an exception for ladder polymers, which show end-limited hole

(58) Zachmanoglou, E. C.; Thoe, D. W. *Introduction to Partial Differential Equations with Applications*; Dover Publications: New York, 1986.
(59) Tanaka, M.; Yoshida, H.; Ogasawara, M. *J. Phys. Chem.* **1991**, *95*, 955–960.
(60) Yoshida, H.; Ogasawara, M.; Tanaka, M. *Radiat. Phys. Chem.* **1992**, *39*, 35–40.
(61) Hoofman, R.; de Haas, M. P.; Siebbeles, L. D. A.; Warman, J. M. *Nature* **1998**, *392*, 54–56.
(62) Grozema, F. C.; Siebbeles, L. D. A.; Warman, J. M.; Seki, S.; Tagawa, S.; Scherf, U. *Adv. Mater.* **2002**, *14*, 228–231.

mobilities, the mobilities determined for most polymers by microwave conductivity, a high-frequency ac technique, are probably averages that emphasize the fast motions within favorable regions. The present results, especially those for pF$_{35}$NI, require displacement over larger distances.

Conclusions

Electrons or holes attached to conjugated polyfluorenes are transported to and react with trap groups at the termini of the chains. End capping is incomplete in these molecules by a varied amount; as much as 40% of pFAPT$_2$ has no APT$_2$ hole trap at either end. A remarkable observation is that, in the more fully capped pFAQ and pFNI molecules, ~70% of the attached electrons reach end-cap traps within a few nanoseconds. Incomplete information about fast charge attachment and bimolecular kinetics between long molecules along with the incompleteness of end capping leaves determination of the rate of charge transport uncertain by a factor of 2. Nevertheless, the present results demonstrate mobilities of ~3.5 × 10^{-3} cm^2/V that are intermediate between the approximately two decade higher values in single pF chains determined by microwave conductivity[13,62] and the lower values usually found in disordered films.[3–9,11] This mobility is uncertain by a factor of 2 because of experimental uncertainties. Additionally, it is based on two end caps per chain. It could be corrected to values up to four times higher if the completeness of end capping were known exactly. At present, the reason for lower mobilities in the present experiments compared to those found by microwave conductivity is not known. While not decisive on this point, the present results are consistent with relatively homogeneous transport without evidence for kinks or other barricades to motion of charges. Some of the difference may reflect the long distance of charge transport in the present experiments. An appealing explanation for lower mobility is slower polaron motion due to the polarity of THF used here as compared to nonpolar fluids used for microwave conductivity. Such an effect of polarity, important information for theories of charge transport and our understanding of the nature of charges in conjugated polymers, to our knowledge, has not been reported. An important challenge will be adaptation of the present methods to measurement in less polar or more polar media.

For pF chains, determinations of persistence lengths of 7–17 nm[20,21] inform us that the chains are not straight over distances longer than 7–17 nm. But the roughly single-exponential transport observed here by 70% of attached charges is probably inconsistent with the presence of kinks or other defects[14,15,22–25,63] that halt or drastically slow the motion of diffusing charges. It would be consistent with description[20,21] of pF's with models based on wormlike chains.[64] A collapse from extended chains into globular structures,[25,63] as reported for PPVs, would be difficult to reconcile with the present observations, which point to extended structures.

The term "molecular wires" conjures images of the capability for directed transport of charges over very long distances. By observing charge transport over substantial distances within single chains, the experiments reported here provide some support for this vision, but leave many questions. Questions of long distance transport of charge and even the meaning of the term "molecular wires" to describe conjugated polymers will only be solved with simultaneous understanding of both the transport and the structures in which it occurs. This is a broad complex problem, but one of substantial importance in a field with promise.

Supporting Information Available: GPC and NMR spectra, time-resolved transient absorption spectra, cyclic voltammograms, transient absorption vs time at end cap wavelengths, a more detailed pictorial description of the kinetic scheme and illustrations of random walk. This material is available free of charge via the Internet at http://pubs.acs.org.

JA800426Z

(63) Grey, J. K.; Kim, D. Y.; Donley, C. L.; Miller, W. L.; Kim, J. S.; Silva, C.; Friend, R. H.; Barbara, P. F. *J. Phys. Chem. B* **2006**, *110*, 18898–18903.

(64) Kratky, O.; Porod, G. *Recl. Trav. Chim. Pays-Bas* **1949**, *68*, 1106–1123.